The Astrophysical Journal, 613:L85–L88, 2004 October 1


# THE HOT AND COLD SPOTS IN THE *WILKINSON MICROWAVE ANISOTROPY PROBE* DATA ARE NOT HOT AND COLD ENOUGH

David L. Larson[1] and Benjamin D. Wandelt[1,2,3]
*Received 2004 April 2; accepted 2004 August 23; published 2004 September 3*

## ABSTRACT

This Letter presents a frequentist analysis of the hot and cold spots of the cosmic microwave background data collected by the *Wilkinson Microwave Anisotropy Probe* (*WMAP*). We compare the *WMAP* temperature statistics of extrema (number of extrema, mean excursion, variance, skewness, and kurtosis of the excursion) to Monte Carlo simulations. We find that on average, the local maxima (high temperatures in the anisotropy) are too cold and the local minima are too warm. In order to quantify this claim we describe a two-sided statistical hypothesis test that we advocate for other investigations of the Gaussianity hypothesis. Using this test we reject the isotropic Gaussian hypothesis at more than 99% confidence in a well-defined way. Our claims are based only on regions that are outside the most conservative *WMAP* foreground mask. We perform our test separately on maxima and minima and on the north and south ecliptic and Galactic hemispheres and reject Gaussianity at above 95% confidence for almost all tests of the mean excursions. The same test also shows the variance of the maxima and minima to be low in the ecliptic north (99% confidence) but consistent in the south; this effect is not as pronounced in the Galactic north and south hemispheres.

*Subject heading:* cosmic microwave background

## 1. INTRODUCTION

The *Wilkinson Microwave Anisotropy Probe* (*WMAP*) data provide the most detailed data on the full sky cosmic microwave background (CMB) to date. This information about the initial density fluctuations in the universe allows us to test the cosmological standard model at unprecedented levels of detail (Bennett et al. 2003a). A question of fundamental importance to our understanding of the origins of these primordial seed perturbations is whether the CMB radiation is really an isotropic and Gaussian random field, as generic inflationary theories predict (Starobinsky 1982; Guth & Pi 1982; Bardeen et al. 1983).

A natural way to study the CMB is to look at the local extrema. This was initially suggested because the high signal-to-noise ratio at the hot spots means that they would be detected first (Sazhin 1985; Zabotin & Naselsky 1985; Vittorio & Juszkiewicz 1987; Bond & Efstathiou 1987). Heavens & Sheth calculate analytically the two-point correlation function of the local extrema (Heavens & Sheth 1999). In addition, extrema trace topological properties of the temperature map; this makes them good candidates for study (Wandelt et al. 1998).

We pursue this investigation by simulating Gaussian Monte Carlo CMB skies and comparing the *WMAP* data to those simulations. We choose several statistics and then check to see if the *WMAP* statistics lie in the middle of the Monte Carlo distributions of statistics. We present results on the one-point functions of the local extrema: their number, mean excursion, and variance, and skewness and kurtosis of the excursion.

The literature contains many other searches for non-Gaussianity, in the *WMAP* data and other CMB experiments. For example, Vielva et al. detect non-Gaussianity in the three- and four-point wavelet moments (Vielva et al. 2004), Chiang et al. detect it in phase correlations between spherical harmonic coefficients (Chiang et al. 2003; see also Chiang et al. 2002, 2004), and Park finds it in the genus Minkowski functional (Park 2004). Eriksen et al. find anisotropy in the *n*-point functions of the CMB in different patches of the sky (Eriksen et al. 2004). Others discuss possible methods of detecting non-Gaussianity. Aliaga et al. look at studying non-Gaussianity through spherical wavelets and "smooth tests of goodness of fit" (Aliaga et al. 2003). Cabella et al. review three methods of studying non-Gaussianity: through Minkowski functionals, spherical wavelets, and the spherical harmonics (Cabella et al. 2004). They propose a way to combine these methods.

Komatsu et al. discuss a fast way to test the bispectrum for primordial non-Gaussianity in the CMB (Komatsu 2003a) and do not detect it (Komatsu et al. 2003b). Finally, Gaztañaga et al. find the CMB to be consistent with Gaussianity when considering the two- and three-point functions (Gaztañaga & Wagg 2003; Gaztañaga et al. 2003). To this work, we add a strong detection of non-Gaussianity based on generic features: the local extrema.

The Letter is laid out as follows. The next section discusses our method for making Monte Carlo simulations of the CMB sky and calculating statistics on both the simulations and the *WMAP* data. It also explains our statistical tests. Section 3 describes our results. We conclude in § 4.

## 2. METHOD

We test the *WMAP* data of the CMB sky by comparing the one-point statistics of its extrema to those same statistics on several sets of Monte Carlo–simulated Gaussian skies. Our null hypothesis is that the statistics of the *WMAP* data are drawn from the same probability density function (PDF) as the statistics of the Monte Carlo skies. If some *WMAP* one-point statistic falls lower or higher than most of the Monte Carlo statistics, this indicates that our hypothesis may be false.

We examine several inputs to our Monte Carlo simulation to see how those change the Monte Carlo distribution of one-point statistics around the *WMAP* one-point statistics. We start very generally, looking at different frequency bands and ga-

[1] Department of Physics, University of Illinois at Urbana-Champaign, Loomis Laboratory of Physics, MC-704, 1110 West Green Street, Urbana, IL 61801; dlarson1@uiuc.edu.

[2] Department of Astronomy, University of Illinois at Urbana-Champaign, 103 Astronomy Building, 1002 West Green Street, Urbana, IL 61801; bwandelt@uiuc.edu.

[3] 2003/2004 NCSA faculty fellow.

lactic masks, and then narrow our search. Initially, we look at simulations including the three frequency bands (Q, V, and W) and the three published galactic masks for the *WMAP* data. Then we check to see if changing to a different published theoretical power spectrum affects our results. Finally, we look for anisotropy between the statistics of the ecliptic and Galactic north and south hemispheres.

### 2.1. *Monte Carlo Simulation*

A general outline of our Monte Carlo simulation process follows. Each set of skies is labeled by its theoretical power spectrum, frequency band (Q, V, or W), and galactic mask. The frequency band determines both the (azimuthally averaged) beam shape function and the noise properties on the sky. The simulated CMB skies are created as follows:

1. A Gaussian CMB sky is created with SYNFAST, using a power spectrum and a beam function. The HEALPix[4] pixelization of the sphere is used, with $N_{\rm side} = 512$.
2. Random Gaussian noise is added to the sky (at each pixel) according to the published noise characteristics of the band being simulated. The *WMAP* radiometers are characterized as having white Gaussian noise (Jarosik et al. 2003).
3. The monopole and dipole moments of the sky (outside of the chosen galactic mask) are removed.

We make no attempt to simulate any foregrounds, including the galaxy; our analysis ignores data inside a galactic mask and uses the cleaned maps published on LAMBDA (Legacy Archive for Microwave Background Data Analysis; NASA 2003).

For each Monte Carlo set, one of four power spectra is used. These are the power spectra published by the *WMAP* team on LAMBDA (NASA 2003). We primarily use the best-fit (bf) theoretical power spectrum to a cold dark matter universe with a running spectral index using the *WMAP*, Cosmic Background Imager (CBI), Arcminute Cosmology Bolometer Array Receiver (ACBAR), Two-Degree Field, and Ly$\alpha$ data. In addition, we check the unbinned power spectrum (w) directly measured by *WMAP*, the power-law (pl) theoretical power spectrum fitted to *WMAP*, CBI, and ACBAR, and a running index (ri) theoretical power spectrum fitted to *WMAP*, CBI, and ACBAR. See Spergel et al. (2003), Bennett et al. (2003a), and NASA (2003) for more information.

The galactic masks used are the Kp0, Kp2, and Kp12 masks published by the *WMAP* team (Bennett et al. 2003b). To check for differences between the north and south ecliptic hemispheres, we define additional masks that extend the Kp0 galactic mask to block either the north or the south hemisphere as well. For example, the ecliptic south (ES) mask blocks the northern ecliptic sky as well as the galaxy. As a control, we also extend the Kp0 mask for galactic north and south hemispheres (GN and GS) to bring the total number of masks up to seven: Kp0, Kp2, Kp12, GS, GN, ES, and EN. We use the same masking and dipole removal procedure for the *WMAP* data as for the Monte Carlo skies.

The *WMAP* data that we use are the cleaned, published maps. They are published by channel, so we calculate an *unweighted* average over (for example) all four W-band channels to get a map for the W band. The noise variance is calculated accordingly. We compute an unweighted average of the maps so that we can combine the *WMAP* beam functions through a simple average.

[4] See http://www.eso.org/science/healpix.

### 2.2. *Analysis and Hypothesis Test*

Our analysis of both the Monte Carlo and the *WMAP* skies involves the following: We find the local maxima and minima of the HEALPix grid using HOTSPOT. Then we discard the extrema blocked by the galactic mask. We calculate the statistics (number, mean, variance, skewness, and kurtosis) on the temperatures of the maxima and minima and then statistically analyze the significance of the position of the *WMAP* statistic among the Monte Carlo statistics. Because we consider only the one-point statistics, we consider only the temperature values, not their locations.

We calculate our five statistics for the maxima and minima separately. The two statistics that are typically negative for the minima, the mean and skewness, are multiplied by $-1$ in our results, to make comparison with the maxima statistics more clear.

For the rest of this section, we explain our analysis of the statistics in detail. To simplify the discussion, we consider the analysis of only one statistic on either maxima or minima, as we analyze the results for each statistic separately.

Our Monte Carlo simulations are binomial trials, where the statistic calculated on a simulation can lie either above or below the *WMAP* statistic. It lies below the *WMAP* statistic with probability $p$, and for some set of $n$ trials, $i$ of the trials will have statistics below the *WMAP* statistic. Given $p$, the probability of $i$ is $P(i|p) = [n!/i!(n-i)!]\,p^i(1-p)^{n-i}$. The value $\hat{p} \equiv i/n$ is both an unbiased and a maximum likelihood estimator of $p$.

We are interested in whether $p$ is near 0 or 1, since that indicates that our hypothesis—that the *WMAP* statistic came from the same PDF as the Monte Carlo statistics—may be false. Because we do not have an alternative distribution for the *WMAP* statistic that we can test against the Monte Carlo distribution, we do not test our hypothesis as phrased. We only look at a hypothesis $H_0$ that claims $p$ is in some interval, $p \in (\alpha/2, 1-\alpha/2)$, where we have arbitrarily chosen $\alpha = 0.05$.

We devise a statistical test of this hypothesis. Given our experimental result $i$, we construct the $1-\alpha = 95\%$ symmetric confidence interval for $p$, as described in Kendall & Stuart (1973). If this confidence interval lies entirely within the interval $[0, \alpha/2]$ or entirely within $[1-\alpha/2, 1]$, then we reject our hypothesis $H_0$. We reject $H_0$ for no values of $i$ when $n = 99$, for $0 \le i \le 15$ or $985 \le i \le 1000$ when $n = 1000$, and for $0 \le i \le 103$ or $4897 \le i \le 5000$ when $n = 5000$.

This interval is a "95%" confidence interval in the following frequentist (non-Bayesian) sense. Suppose we repeat the experiment (with the same number of Monte Carlo runs and the same *WMAP* data) many times and get many values of $i$. We recalculate the confidence intervals each time, for each particular value of $i$. Ninety-five percent of the confidence intervals that we calculate will contain the true value of $p$.

Our test is biased in favor of $H_0$. Let $H_1$ be the alternative hypothesis $p \in [0, \alpha/2] \cup [1-\alpha/2, 1]$. Then, for some values of $p$ where $H_1$ is true (for example, $p = 0.02$, $n = 1000$), our test will choose $H_0$ more often than $H_1$, given that $i$ is a random variable with probability $P(i|p)$. If desired, we can make the test unbiased by changing our value of $\alpha$ in the hypotheses $H_0$ and $H_1$ but keeping the test (range of $i$ for which $H_0$ is accepted) the same.

For $n = 1000$, we have an unbiased test if $\alpha = 0.0313$, and for $n = 5000$, we have an unbiased test if $\alpha = 0.0415$. Note

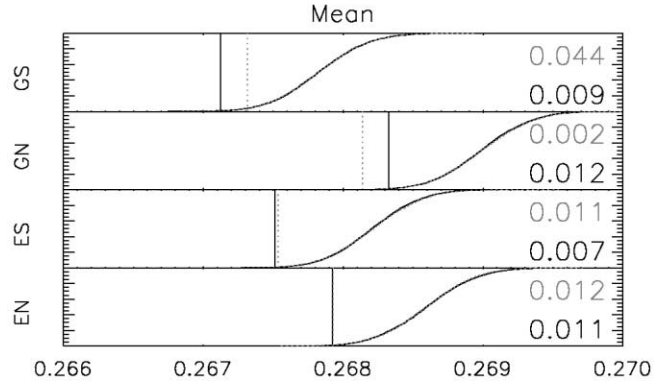


FIG. 1.—Cumulative distribution functions (CDFs) of mean temperature value (in units of millikelvins) of the local extrema, found in sets of 5000 Monte Carlo simulations for four galactic masks: GS, GN, ES, and EN. Best-fit power spectrum and W-band data are used. Means of the minima are negated for comparison. Maxima CDF is dotted, while minima CDF is solid. Note their visual similarity. Statistics measured on *WMAP* data are shown as two vertical lines, dotted for maxima and solid for minima. Numbers on the right are the same probabilities as in Table 1; for each pair, probability for the maxima is higher on the page.

that these values are less than $\alpha = 0.05$. For any value of $p$, these tests are at least as likely to choose the correct hypothesis as the incorrect one. This is a 50% confidence, as opposed to our previous 95% confidence. This interpretation of the test does not change our results; it merely provides the different perspective that our test may be considered an unbiased 96.9% test for $n = 1000$ or an unbiased 95.9% test for $n = 5000$.

## 3. RESULTS

We display our results in Figure 1 and Table 1. The figure shows where the means of the *WMAP* maxima (and minima) lie in the Monte Carlo cumulative distribution functions for that statistic. The table contains our estimates $\hat{p}$ of $p$. When the result rejects the hypothesis $H_0$, this is noted with a footnote.

We find that the mean temperature of the *WMAP* extrema, and in some cases the variance, differs significantly from the simulations, but the number of extrema, skewness, and kurtosis are modeled fairly well by the simulations. There is ecliptic north-south asymmetry in the variance of the extrema.

For the mean, all of our results reject our hypothesis $H_0$ for the power law and running index power spectra, and all four of our results for the ecliptic north and south hemispheres reject $H_0$ when $n = 1000$ and 5000. Since the statistics for the minima are negated, this means that the *WMAP* maxima are too cold and the *WMAP* minima are too hot. This is a very significant result, regardless of whether our tests are considered 95% tests biased away from detection or a 96.9% and a 95.9% test.

Even more significant are two 99% ($\alpha = 0.01$) level detections. In Table 1, they are rows bf, W, GN, max, and mean, and bf, W, EN, max, and variance. For this level of detection, we only accept values of $i$ where $0 \le i \le 12$ or $4988 \le i \le 5000$. No 99% confidence detection was possible with only 1000 iterations.

Using our initial 99 simulations, we find qualitatively low mean excursions in the Q and W bands, but not the V band. We chose the W band to examine further because it had the best signal-to-noise ratio, and it had the least chance of foregrounds outside the Kp0 mask that we use in our final analysis.

It has been suggested (Eriksen et al. 2004) that there is statistical anisotropy between the ecliptic north and south hemispheres. We see this in the variance of the extrema temperatures. The ecliptic north hemisphere has a statistically low variance (in one case at the 99% level), while the ecliptic south is normal. To compare, we find the galactic north to be slightly low while the south is again normal.

TABLE 1

ESTIMATED PROBABILITIES $\hat{p}$ OF THE CMB STATISTICS BEING LESS THAN THE VALUE MEASURED BY *WMAP*, BASED ON SEVERAL MONTE CARLO SAMPLINGS OF THOSE STATISTICS

| Identifier | 0 | 1 | 2 | 3 | 4 | 5 |
|---|---|---|---|---|---|---|
| bf, Q, Kp0, max ..... | 0.374 | 0.000 | 0.030 | 0.566 | 0.889 | 99 |
| bf, Q, Kp0, min ..... | 0.010 | 0.000 | 0.232 | 0.919 | 0.707 | ... |
| bf, Q, Kp2, max ..... | 0.333 | 0.000 | 0.152 | 0.545 | 0.899 | 99 |
| bf, Q, Kp2, min ..... | 0.010 | 0.000 | 0.293 | 0.919 | 0.768 | ... |
| bf, Q, Kp12, max ..... | 0.020 | 0.000 | 0.576 | 0.929 | 1.000 | 99 |
| bf, Q, Kp12, min ..... | 0.000 | 0.000 | 0.798 | 0.919 | 1.000 | ... |
| bf, V, Kp0, max ..... | 0.091 | 0.616 | 0.182 | 0.495 | 0.848 | 99 |
| bf, V, Kp0, min ..... | 0.030 | 0.182 | 0.303 | 0.990 | 0.960 | ... |
| bf, V, Kp2, max ..... | 0.061 | 0.384 | 0.061 | 0.364 | 0.727 | 99 |
| bf, V, Kp2, min ..... | 0.040 | 0.202 | 0.263 | 1.000 | 0.960 | ... |
| bf, V, Kp12, max ..... | 0.000 | 0.384 | 0.212 | 0.343 | 0.889 | 99 |
| bf, V, Kp12, min ..... | 0.020 | 0.232 | 0.444 | 0.980 | 1.000 | ... |
| bf, W, Kp0, max ..... | 0.475 | 0.000 | 0.141 | 0.364 | 0.475 | 99 |
| bf, W, Kp0, min ..... | 0.414 | 0.000 | 0.343 | 0.879 | 0.646 | ... |
| bf, W, Kp2, max ..... | 0.495 | 0.000 | 0.131 | 0.182 | 0.283 | 99 |
| bf, W, Kp2, min ..... | 0.293 | 0.000 | 0.323 | 0.808 | 0.616 | ... |
| bf, W, Kp12, max ..... | 0.434 | 0.000 | 0.242 | 0.313 | 0.253 | 99 |
| bf, W, Kp12, min ..... | 0.364 | 0.010 | 0.505 | 0.707 | 0.737 | ... |
| pl, W, Kp0, max ..... | 0.427 | 0.002* | 0.129 | 0.461 | 0.410 | 1000 |
| pl, W, Kp0, min ..... | 0.377 | 0.000* | 0.224 | 0.880 | 0.704 | ... |
| ri, W, Kp0, max ..... | 0.388 | 0.000* | 0.216 | 0.285 | 0.310 | 1000 |
| ri, W, Kp0, min ..... | 0.396 | 0.000* | 0.406 | 0.821 | 0.618 | ... |
| w, W, GS, max ..... | 0.633 | 0.023 | 0.362 | 0.045 | 0.304 | 1000 |
| w, W, GS, min ..... | 0.685 | 0.007* | 0.981 | 0.247 | 0.213 | ... |
| w, W, GN, max ..... | 0.436 | 0.000* | 0.168 | 0.504 | 0.159 | 1000 |
| w, W, GN, min ..... | 0.243 | 0.006* | 0.060 | 0.832 | 0.610 | ... |
| w, W, ES, max ..... | 0.607 | 0.010* | 0.869 | 0.103 | 0.429 | 1000 |
| w, W, ES, min ..... | 0.176 | 0.003* | 0.923 | 0.244 | 0.152 | ... |
| w, W, EN, max ..... | 0.470 | 0.011* | 0.019 | 0.416 | 0.119 | 1000 |
| w, W, EN, min ..... | 0.702 | 0.005* | 0.067 | 0.958 | 0.861 | ... |
| bf, W, GS, max ..... | 0.603 | 0.044 | 0.240 | 0.152 | 0.434 | 5000 |
| bf, W, GS, min ..... | 0.641 | 0.009* | 0.852 | 0.405 | 0.284 | ... |
| bf, W, GN, max ..... | 0.371 | 0.002* | 0.091 | 0.648 | 0.284 | 5000 |
| bf, W, GN, min ..... | 0.209 | 0.012* | 0.035 | 0.883 | 0.697 | ... |
| bf, W, ES, max ..... | 0.560 | 0.011* | 0.472 | 0.198 | 0.487 | 5000 |
| bf, W, ES, min ..... | 0.151 | 0.007* | 0.586 | 0.376 | 0.253 | ... |
| bf, W, EN, max ..... | 0.436 | 0.012* | 0.002* | 0.529 | 0.188 | 5000 |
| bf, W, EN, min ..... | 0.668 | 0.011* | 0.011* | 0.960 | 0.869 | ... |

NOTES.—The identifier column provides the power spectrum, band, and mask used and whether the statistics are for minima or maxima. Power spectra are best fit (bf), power law (pl), running index (ri), or measured unbinned *WMAP* (w). Columns labeled 0 through 4 give an unbiased estimate of the *WMAP* statistic's position among the sorted Monte Carlo sample statistics. The statistic in column 0 is the number of hot spots. The other columns correspond to: 1, mean; 2, variance; 3, skewness; and 4, kurtosis of extrema temperature values. (For minima, mean and skewness statistics are negated before estimating the probability of the *WMAP* statistic being lower.) Column 5 gives the number of Monte Carlo samples calculated. Probabilities that indicate that "the true value of $p$ is at least 95% likely to be within 0.025 of either 0 or 1" are marked with an asterisk. The table shows that the data fall low in the mean temperature distribution for almost every set of simulations.

## 4. CONCLUSION

In this Letter we generate simulated CMB skies. We choose several statistics and calculate them on both the simulations and the *WMAP* sky. We hypothesize that the *WMAP* statistics are drawn from the same distribution as the simulations' statistics, since we have attempted to accurately simulate the CMB sky. If the *WMAP* statistic is higher or lower than most of the

simulations' statistics, this indicates that the *WMAP* statistic's underlying position $p \in [0, 1]$ in the distribution of Monte Carlo statistics is close to 0 or 1. If we are 95% confident that $p$ is within 0.025 of 0 or 1, then we claim that the probability of the *WMAP* statistic happening by chance is sufficiently small to reject the hypothesis.

We find the *WMAP* data to have maxima that are significantly colder and minima that are significantly warmer than predicted by Monte Carlo simulation. For almost all simulations, we have 95% confidence that the mean of the *WMAP* hot spots or cold spots is in a 5% tail of the Monte Carlo distribution. In one case, we are 99% confident that the maxima statistic is in a 1% tail. Since we find the same lack of extreme temperature when we use the directly measured *WMAP* power spectrum, we are not simply restating that the *WMAP* power spectrum has a lack of power at large angular scales. The effect is independent of the galactic mask or power spectrum used.

We also find some anisotropy between the ecliptic north and south hemispheres. The *WMAP* data in the northern hemisphere have a low variance statistic (95% confident that the variance statistic is in a 5% tail). In one case, we are 99% confident that the variance of the maxima is in a 1% tail. There is less asymmetry between the north and south galactic hemispheres.

Our results may not be a detection of primordial non-Gaussianity. They could still be an effect of the *WMAP* instrument or data pipeline not modeled in our simulations or an as yet undiscovered foreground. Our result is still highly significant. We have detected something, whether it is primordial non-Gaussianity or some other effect in the data. Having anomalous mean temperature values for the maxima and minima in both the north and the south ecliptic hemispheres is unlikely to occur if the *WMAP* data were consistent with theoretical expectations. We will present a complete treatment of the one- and two-point extrema statistics for the *WMAP* data set in a future publication.

Some of the results in this Letter have been derived using the HEALPix package (Górski et al. 1999). We would like to thank D. Spergel and O. Doré for reading our manuscript. This work was partially supported by the University of Illinois.

REFERENCES

Aliaga, A., Martínez-González, E., Cayón, L., Argueso, F., Sanz, J., Barreiro, R., & Gallegos, J. 2003, NewA Rev., 47, 907
Bardeen, J. M., Steinhardt, P. J., & Turner, M. S. 1983, Phys. Rev. D, 28, 679
Bennett, C., et al. 2003a, ApJS, 148, 1
———. 2003b, ApJS, 148, 97
Bond, J. R., & Efstathiou, G. 1987, MNRAS, 226, 655
Cabella, P., Hansen, F., Marinucci, D., Pagano, D., & Vittorio, N. 2004, Phys. Rev. D, 69, 063007
Chiang, L.-Y., Coles, P., & Naselsky, P. 2002, MNRAS, 337, 488
Chiang, L.-Y., Naselsky, P., & Coles, P. 2004, ApJ, 602, L1
Chiang, L.-Y., Naselsky, P. D., Verkhodanov, O. V., & Way, M. J. 2003, ApJ, 590, L65
Eriksen, H. K., Hansen, F. K., Banday, A. J., Górski, K. M., & Lilje, P. B. 2004, ApJ, 605, 14
Gaztañaga, E., & Wagg, J. 2003, Phys. Rev. D, 68, 021302
Gaztañaga, E., Wagg, J., Multamäki, T., Montaña, A., & Hughes, D. H. 2003, MNRAS, 346, 47
Górski, K. M., Hivon, E., & Wandelt, B. D. 1999, in Evolution of Large-Scale Structure: From Recombination to Garching, ed. A. J. Banday, R. K. Sheth, & L. A. N. da Costa (Enschede: PrintPartners Ipskamp), 37
Guth, A. H., & Pi, S.-Y. 1982, Phys. Rev. Lett., 49, 1110
Heavens, A. F., & Sheth, R. K. 1999, MNRAS, 310, 1062
Jarosik, N., et al. 2003, ApJS, 148, 29
Kendall, M. G., & Stuart, A. 1973, The Advanced Theory of Statistics: Inference and Relationship (3rd ed.; New York: Hafner)
Komatsu, E., Spergel, D. N., & Wandelt, B. D. 2003a, ApJL, submitted (astro-ph/0305189)
Komatsu, E., et al. 2003b, ApJS, 148, 119
NASA. 2003, Legacy Archive for Microwave Background Data Analysis, http://lambda.gsfc.nasa.gov
Park, C. 2004, MNRAS, 349, 313
Sazhin, M. V. 1985, MNRAS, 216, 25P
Spergel, D. N., et al. 2003, ApJS, 148, 175
Starobinsky, A. A. 1982, Phys. Lett. B, 117, 175
Vielva, P., Martínez-González, E., Barreiro, R. B., Sanz, J. L., & Cayón, L. 2004, ApJ, 609, 22
Vittorio, N., & Juszkiewicz, R. 1987, ApJ, 314, L29
Wandelt, B. D., Hivon, E., & Górski, K. M. 1998, in Proc. 33rd Recontres de Moriond, Fundamental Parameters in Cosmology, ed. J. Trân Thanh Vân et al. (Paris: Editions Frontières), 237
Zabotin, N. A., & Naselsky, P. D. 1985, Soviet Astron., 29, 614